Available online at www.sciencedirect.com
SCIENCE DIRECT
Journal of Molecular Catalysis A: Chemical 243 (2006) 60–67
JOURNAL OF MOLECULAR CATALYSIS A: CHEMICAL
www.elsevier.com/locate/molcata

Enhanced photocatalytic activity of TiO_2 by doping with Ag for degradation of 2,4,6-trichlorophenol in aqueous suspension

S. Rengaraj, X.Z. Li *

Department of Civil and Structural Engineering, The Hong Kong Polytechnic University, Hong Kong, China

Received 19 May 2005; received in revised form 2 August 2005; accepted 2 August 2005
Available online 19 September 2005

Abstract

A series of Ag-TiO_2 nanocatalysts were synthesized by a sol–gel method with a doping content up to 2 wt%-Ag. The physico-chemical characteristics of the synthesized catalysts were characterized by X-ray diffraction, X-ray photoelectron emission spectroscopy, transmission electron microscopy, UV–vis absorption spectrometer, and optical ellipsometry to study the influence of the Ag content on the surface properties, optical absorption and other characteristics of the photocatalysts. The photocatalytic activity of the Ag-TiO_2 was evaluated in the 2,4,6-trichlorophenol (TCP) degradation and mineralization in aqueous solution under UV-A illumination. The experiments demonstrated that TCP was effectively degraded by more than 95% within 120 min. It was confirmed that the presence of Ag on TiO_2 catalysts could enhance the photocatalytic oxidation of TCP in aqueous suspension and the experimental results showed that the kinetics of TCP degradation follows a pseudo-first-order kinetic model. It was found that an optimal dosage of 0.5 wt% Ag in TiO_2 achieved the fastest TCP degradation under the experimental conditions. The experimental results of TCP mineralization indicated while total organic carbon was reduced by a high portion of up to 80% within 120 min, most chlorine on TCP was more quickly converted to chloride within the first 40 min. On the basis of various characterizations of the photocatalysts, the reactions involved to explain the photocatalytic activity enhancement due to Ag doping include a better separation of photogenerated charge carriers and improved oxygen reduction inducing a higher extent of degradation of aromatics.

Keywords: Ag doping; Photodegradation; Sol–gel; TiO_2; 2,4,6-Trichlorophenol; UV light

1. Introduction

Research into water purification using advanced oxidation technologies is expanding steadily. The majority of investigations on the chloroaromatic compounds are based on photochemical and photocatalytical methods [1,2]. During the last two decades there has been a growing concern related to the environmental and health impacts and environmental damage due to chlorinated organic compounds [3]. The presence of chlorinated aromatic compounds in the aqueous environment is a consequence of the widespread use of chlorinated organics in a variety of industrial processes. These substances are persistent and have been shown to accumulate in the environment [4]. Adverse effects on the human nervous system have been recently reported and have been linked to many health disorders [5]. Therefore, it is important to find innovative and cost-effective methods for the safe and complete destruction of chlorinated organics such as chlorophenols.

The conventional treatment technologies include biological treatment, adsorption technology, air stripping and incineration. However, those techniques have some limitations and disadvantages. For example biological treatment for the decomposition of many chlorinated phenols have proven inefficient since chlorinated phenols are resistant to biodegradation within an acceptable time period and tend to accumulate in sediments [3,5,6]. Chlorophenols do not undergo direct sunlight photolysis in the natural environment since they only absorb light below 290 nm [7]. Therefore, the current trend in treatment has moved from phase transfer to destruction of pollutants such as advanced oxidation processes (AOPs). These techniques involve reactive free radical species for non-selective mineralization of organic compounds to harmless end products [8]. Photocatalysis as an abatement method for the degradation of these compounds has been paid promising attention by researchers during the past two

* Corresponding author. Tel.: +852 2766 6016; fax: +852 2334 6389.
E-mail address: cexzli@polyu.edu.hk (X.Z. Li).

1381-1169/$ – see front matter © 2005 Elsevier B.V. All rights reserved.
doi:10.1016/j.molcata.2005.08.010

decades [4]. Particularly owing to its excellent photocatalytic activity, TiO_2 has been widely studied as an effective photocatalyst for environment purification. Numerous studies have been focused on its unique performance in photocatalytic degradation of toxic organics. However, for practical application, the photocatalytic activity of TiO_2 needs a further improvement. For this reason, a lot of efforts have been made to dope with some transition and noble metals. Recently, researches have demonstrated that the addition of certain metals, such as platinum (Pt), palladium (Pd), gold (Au) and some semiconductors can effectively enhance the degradation efficiency of photocatalytic reaction [9]. The enhancement of photodegradation efficiency by the addition of metals like silver (Ag) may be attributed to the rapid transfer of the photogenerated electrons from the semiconductors to the metal particles, resulting in the effective separation of the electrons and holes [10].

This present work focuses on the photocatalytic properties of Ag-TiO_2 catalysts prepared by an ultrasonic-assisted sol–gel technique. These catalysts were tested in the photocatalytic degradation of 2,4,6-trichlorophenol (TCP). The influence of the Ag content on the photocatalytic activity, surface properties, optical absorption and other characteristics of the photocatalysts have been investigated.

2. Experimental

2.1. Materials

Tetra-*n*-butyl titanate ($Ti(O{-}Bu)_4$) and silver nitrate ($AgNO_3$) with analytical grade were purchased from Aldrich Chemical Company and used as titanium and silver sources for preparation of TiO_2 and Ag-TiO_2 photocatalysts. TCP (2,4,6-trichlorophenol) was also obtained from Aldrich Chemical Company with analytical grade and used without further purification. Deionzied and distilled water was used for preparation of all solutions.

2.2. Preparation of photocatalyst

A series of Ag-TiO_2TiO_2 samples were prepared by the ultrasonic-assisted sol–gel method. In which 21 mL of $Ti(O{-}Bu)_4$ was added into 80 mL of absolute ethanol, and the resulting $Ti(O{-}Bu)_4$–ethanol solution was stirred in an ice bath, and then 2 mL of water and 0.2 mL of HNO_3 (50%) were added to another 80 mL of ethanol to make an ethanol–water–HNO_3 solution. The ethanol–water–HNO_3 solution was slowly added to the $Ti(O{-}Bu)_4$–ethanol solution under stirring and cooling with ice [11]. When the resulting mixture turned to be sol, the $AgNO_3$ solution was dripped in it. The dispersion was placed in a supersonic bath, stirred vigorously with a glass-stirring rod, and kept at 25 °C throughout the whole process. After sonification for 30 min, 2 mL of water was dripped into the dispersion gradually until gel was formed. The gel was placed for 24 h at room temperature and then dried at 70 °C under a vacuum condition and then ground. The resulting powder was calcined at 500 °C for 4 h for further studies. A pure TiO_2 sample was also prepared by the same procedure without addition of $AgNO_3$ solution.

2.3. Characterization of photocatalysts

To study the texture and morphology of TiO_2 and Ag-TiO_2 catalysts, the transmission electron microscopy (TEM) and electron dispersive spectroscopy (EDS) was applied using a JEOL JEM – 2011 microscope operated at 200 keV. In which the samples were well dispersed in ethanol by sonication and deposited on a carbon film supported on a copper grid for TEM and EDS analyses.

The crystalline phase of the synthesized TiO_2 and Ag-TiO_2 catalysts was analyzed by X-ray powder diffraction (XRD) using a Philips X- ray diffractometer (PW 3020) with Cu Kα radiation ($\lambda = 0.154060$ nm). The accelerating voltage of 40 kV and an emission current of 30 mA were used.

X-ray photoelectron spectra (XPS) were recorded with a PHI Quantum ESCA microprobe system using a Mg Kα excitation source. Calibration of the spectra was done at the C 1s peak of surface contamination taken at 1253.6 eV. The fitting of XPS curves was analyzed with the software of Multipak 6.0A.

To understand the effect of Ag doping on the band gap of the films, both optical absorbance and spectroscopic ellipsometry measurements were carried out for the Ag-TiO_2 films coated on microscopic slides. Thin films of the TiO_2 and Ag-TiO_2 were prepared by coating corresponding sols onto microscopic slides by dip-coating for optical absorbance properties studies. The optical absorbance spectra were recorded in the spectral range from 1100 to 190 nm by using a Perkin-Elmer λ25 spectrometer. The spectroscopic ellipsometric data were recorded in the spectral range of 0.72–5.2 eV by using a Woollam M2000UI ellipsometer. The spectroscopic ellipsometry data were collected for two different incidence angles of 65 and 75°. The ellipsometer measures the complex ratio of the Fresnel coefficients for s- and p-polarized light and reports the ratio in terms of the ellipsometric parameters psi (ψ) and del (Δ). From the ellipsometry measurements, information about the optical properties of the films can be derived by theoretical simulations by adopting different oscillator models. In this study, the Tauc-Lorentz oscillator model was applied for simulations [12,13]. The theoretical simulations yield the thickness and the dielectric function (DF) of the films. Expressions for the joint density of states were considered for optical transitions from the valance band to the conduction band. From this density of states, the imaginary part of the DF is modeled and then the real part is calculated by fast Fourier transformations to satisfy the causality (Kramers-kronig relation) from this DF. The extinction coefficient of the photocatalyst is eventually determined. Several research groups have successfully used this model to derive the optical properties of the oxide films and more details can be found in the literature [14–16].

2.4. Set up of photocatalytic reactor

All photoreaction experiments were carried out in a photocatalytic reactor system, which consists of a cylindrical borosilicate glass reactor vessel with an effective volume of 250 mL, a cooling water jacket, and a 8-W medium-pressure mercury lamp (Institute of Electric Light Source, Beijing) positioned axially

at the center as a UV-A light source with a main emission at 365 nm. The reaction temperature was kept at 25 °C by cooling water. A special glass frit as an air diffuser was placed at the bottom of the reactor to uniformly disperse air into the solution.

2.5. Experimental procedure

To investigate the effects of Ag doping on the photocatalytic activity of TiO_2, the photocatalytic degradation of TCP was carried out in the TiO_2/Ag-TiO_2 suspension under UV-A irradiation. The reaction suspension was prepared by adding 0.25 g of catalyst into 250 mL of aqueous TCP solution with an initial concentration of 20 mg L^{-1}. Prior to photoreaction, the suspension was magnetically stirred in a dark condition for 30 min to establish an adsorption/desorption equilibrium status. The aqueous suspension containing TCP and photocatalyst were then irradiated under UV-A light with constant aeration. At given time intervals, the analytical samples were taken from the suspension and immediately centrifuged at 4000 rpm for 15 min, and then filtered through a 0.45 μm Millipore filter to remove the particles. The filtrate was analyzed for determining the degree of the TCP degradation.

2.6. Analytical methods

TCP concentration was analyzed by HPLC (Finnigan Mat Spectra system P4000), in which an Atlantis^{TM} C-18 column (5 μm particle size, 150 mm length and 4.6 mm inner diameter) was employed and a mobile phase of acetonitrile/water (65:35, v/v) with 1% acetic acid was used at a flow rate of 0.8 mL min^{-1}. An injection volume of 20 μL was used and the amount of TCP was determined by a UV detector. Total organic carbon (TOC) concentration was determined by a TOC-analyzer (Shimadsu 5000A) equipped with an auto sampler (ASI-5000). The concentration of chloride ion was determined by ion chromatography with a conductivity detector (Shimadzu HIC-6A).

3. Results and discussion

3.1. Characteristics of TiO_2 and Ag-TiO_2 photocatalysts

3.1.1. XRD analysis

The TiO_2 and Ag-TiO_2 samples were examined by XRD and their phase conditions are shown in Fig. 1. The XRD pattern of these samples showed the presence of three main peaks at $2\theta = 25.4$, 37.8, and 48.1°, respectively, regarded as an attributive indication of anatase titania (1 0 1) [17,18]. In addition to the characteristic peak of 1 0 1 plane, diffraction peaks corresponding to rutile titania also appeared on the pattern at $2\theta = 27.5$, 30.8, and 36.4°, respectively. The XRD results indicate that the catalysts have been predominantly crystallized into an anatase phase under this experimental condition.

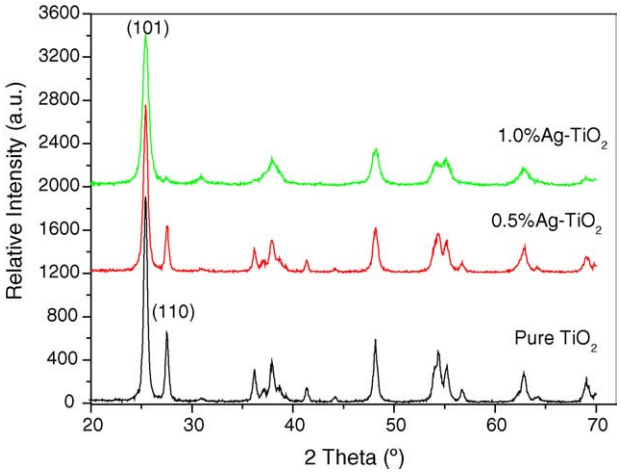

Fig. 1. The XRD photograph of the photocatalysts.

In this investigation, the intensity of the anatase peak at $2\theta = 25.4 \pm 0.1°$ was considered as I_A (A 1 0 1), and the intensity of rutile peak at $2\theta = 27.5 \pm 0.1°$ was considered as I_R (1 1 0). To estimate the fractions of anatase and rutile in the resulting Ag-TiO_2 powder, the weight percentage of the anatase phase, W_A, was calculated using the following equation [19]:

$$W_A = \frac{1}{1 + 1.265(I_R/I_A)} \quad (1)$$

where I_A denotes the intensity of the strongest anatase reflection, and I_R is the intensity of the strongest rutile reflection. For a given sample, the ratio I_A/I_R is independent of fluctuations in diffractometer characteristics.

The calculated results of W_A for all samples are presented in Table 1, which indicate that the 0.5% Ag-TiO_2 and 1% Ag-TiO_2 had the W_A values of 73.80 and 92.39%, higher than that of pure TiO_2 (69.90%). It might be concluded that the content of rutile decreased owing to Ag doping. Ag might be adsorbed on the more active face of rutile preventing thus its further growth. Hence, the anatase phase dominates over rutile. Based on the XRD results, the crystallite sizes of the TiO_2 and Ag-TiO_2 powders were calculated using the Scherrer equation [20] and were found to be between 27 and 43 nm. The lattice parameters "*a*" and "*c*" [21] were determined to be 0.38 and 0.95 nm in all the samples. This might be illustrative of no impact of Ag on the TiO_2 unit cell. Again it might not be isomorphously substituted in the TiO_2 lattice. So it might present as a separate

Table 1
Physical properties of TiO_2 and Ag-TiO_2

Catalysts	Crystal size *D* (nm)	Weight percentage of anatase W_A (%)	$d_{(hkl)a}$	Lattice parameter '*a*' (nm)	Lattice parameter '*c*' (nm)	1 0 1 peak relative intensity (cps)
TiO_2	43.36	69.90	3.5065	0.377	0.951	1875
0.5% Ag-TiO_2	33.73	73.80	3.5038	0.377	0.950	1529
1% Ag-TiO_2	27.57	92.39	3.5154	0.377	0.948	1274

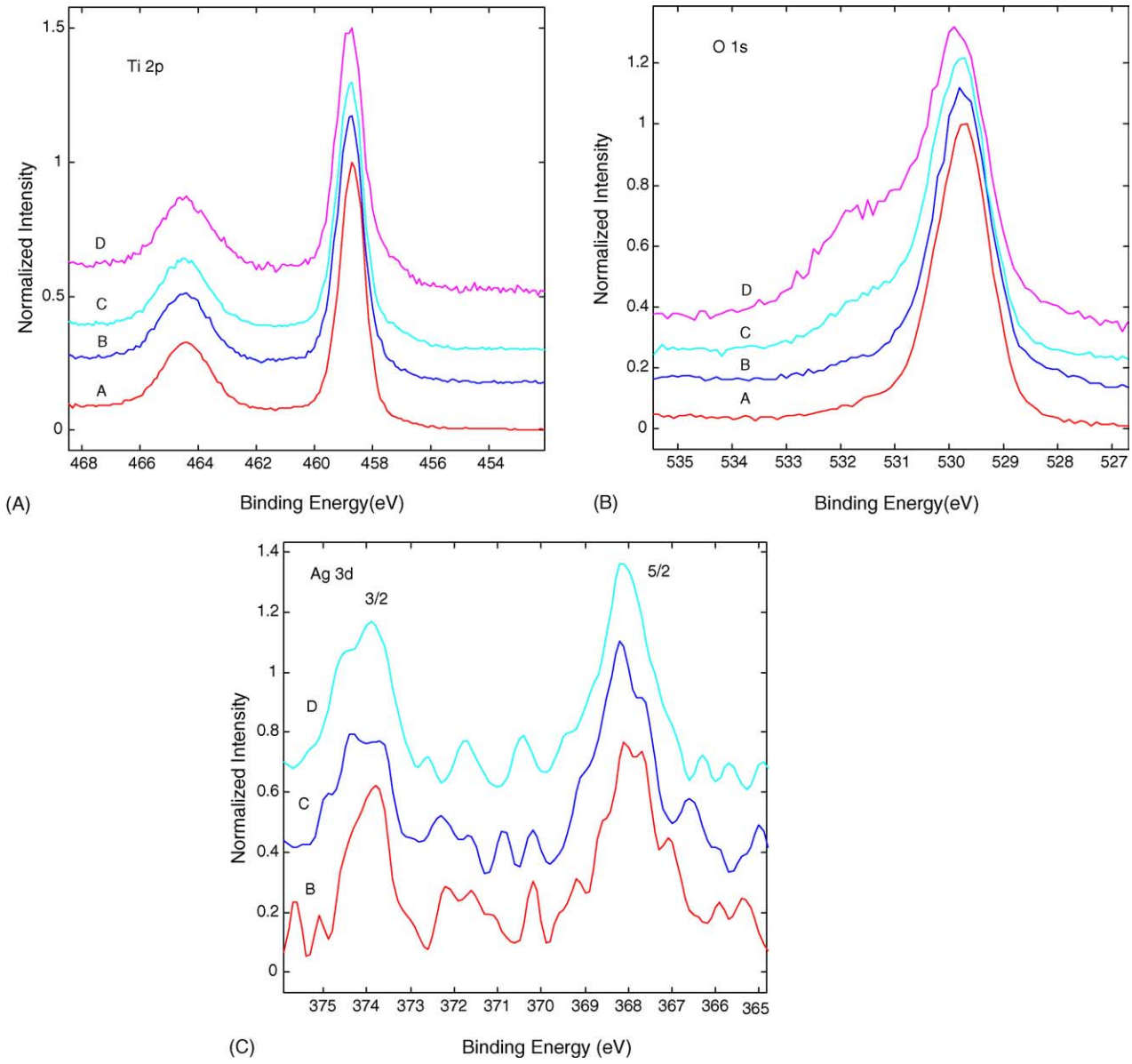

Fig. 2. The XPS spectra of TiO_2 and Ag-TiO_2 samples: (A) Ti 2p, (B) O 1s and (C) Ag 3d.

entity without reacting with the predominant anatase lattice. The results of crystal size (D) and the distance (d_{hkl}) between crystal planes of A 1 0 1 peak in the anatase of all the catalysts are also shown in Table 1. From the data, it can be seen that the TiO_2 powder with Ag doping had only slight changes in its crystal phase, quantum size, and crystal parameter, which should not affect their photoactivity very much.

3.1.2. XPS analysis

The XPS spectra of catalysts are shown in Fig. 2. The results showed that Ti and O elements exist on the surface of the pure TiO_2, while Ti, O and Ag elements occurr on the surface of Ag-TiO_2. According to the high resolution XPS spectra calculated by Multipack 6.0A, the transition involving the Ti 2p, O 1s, and Ag 3d orbital was observed. It can be seen that the Ti 2p XPS peaks of the pure TiO_2 catalyst are narrow and have a binding energy of 458.70 eV (FWHM = 0.95–1.01 eV) attributed to Ti^{4+}. The XPS spectra of the Ag-TiO_2 catalysts showed the presence of two peaks matching Ti^{3+} (457 eV) and Ti^{4+}. The Ti^{3+} might have been formed during oxidation of ethanol by Ag^+ during the preparation. As Ag^+ abstracts an electron from ethanol, the resulting alkoxy radical could act upon by more active Ti^{4+} site on the surface to yield an aldehyde with simultaneous reduction of Ti^{4+} to Ti^{3+}. However, the O 1s XPS spectra showed a wide peak structure for Ag-TiO_2 as illustrated in Fig. 2. The peak at 529.67–529.81 eV (FWHM = 1.15–1.27 eV) for Ag-TiO_2 was an agreement with O 1s electron binding energy for TiO_2 molecules. For pure TiO_2, the O 1s peak with slight asymmetry was narrow and had a binding energy of 529.81 eV (FWHM = 1.15 eV) [10]. In Fig. 2, the Ag 3d peak of Ag-TiO_2 consists of two individual peaks, corresponding to metallic silver (Ag^0-peak area: 75.42%) and silver ion (Ag^+-peak area:

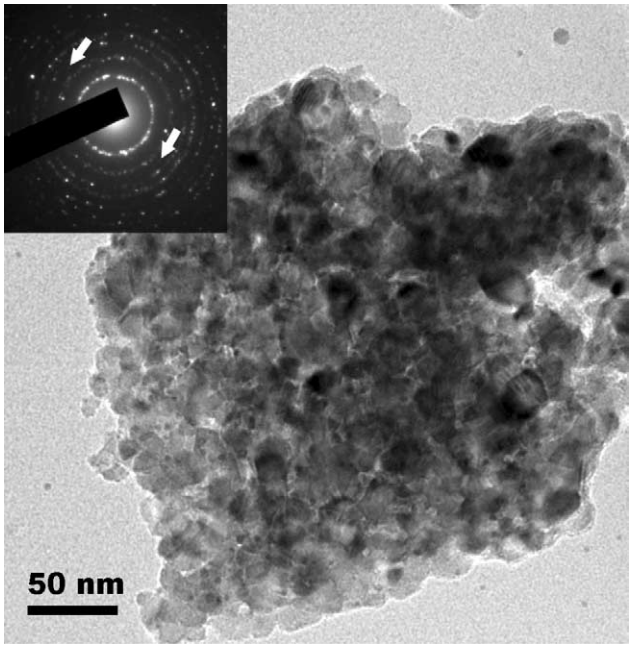

Fig. 3. TEM micrograph of Ag-TiO_2 nanopartciles. [Inserted diffraction pattern indicates that the dominative anatase phase of TiO_2 with traces of brookite TiO_2. Note that the arrows point to diffraction spots giving rise from Ag (2 0 0) planes.]

24.58%), respectively. The peak at 368.04–368.13 eV can be attributed to the Ag^0 [22,23] and the peak at 366.28–366.58 eV to Ag^+. The above results have a strong agreement with the previous literature [23]. In this study, Ag-TiO_2 catalysts were prepared by the sol–gel method, in which $AgNO_3$ was first adsorbed as Ag^+ on the surface of the TiO_2, and then reduced into Ag^0. The different species of Ag on the surfaces of TiO_2 had different photoactivity and optical absorption properties. Therefore, the photoactivity of Ag-TiO_2 samples to UV light was partially caused by the presence of Ag and Ag^+ on the surface of TiO_2.

3.1.3. TEM analysis

The TEM photograph of Ag-TiO_2 hybrid particles are shown in Fig. 3. This figure indicates the bright field image of the nanoparticles. Most of the particles have a size between 20–50 nm in diameter. The inserted figure shows the micro diffraction pattern of a single Ag-TiO_2 particle. This pattern was taken with selected area diffraction corresponding to the spots of crystal silver. Electron diffraction from the nanopartciles confirms that the TiO_2 is in anatase phase, though trace of rutile TiO_2 was detected. The presence of Ag pointed by arrows in the insert, is corresponding to an interplanar distance of 0.207 nm. This value is very close to the value of 0.205 nm of Ag (2 0 0) plane. Furthermore, the electron dispersive spectrum of Ag-TiO_2 is shown in Fig. 4. From this EDS pattern, a very weak signal of Ag and a very strong signal of Ti can be observed. Quantitative analysis of Ag-TiO_2 was found to be about 0.6% of Ag in the mixture in agreement with the added amount. In the meantime, element Cu was also detected, which was from the supporting copper grid.

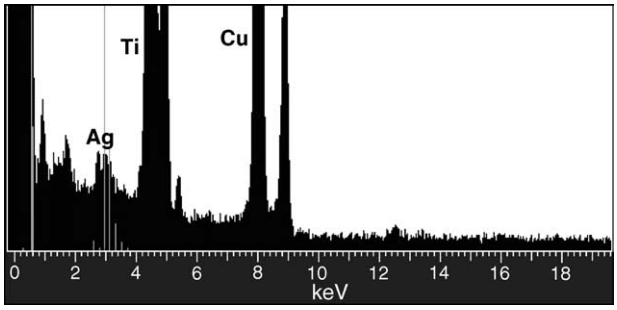

Fig. 4. Electron microdiffraction pattern of Ag-TiO_2 partciles.

3.1.4. Optical absorbance and spectroscopic ellipsometry

The optical absorbance spectra of the Ag-TiO_2 films were measured in the UV–vis region as shown in Fig. 5. It is evidenced that upon increase of the Ag doping content, the absorption edge shifts towards a longer wavelength, which indicates the decrease of the band gap. The typical spectroscopic ellipsometry spectra of a 0.5% Ag-TiO_2 sample coated on a microscopic slide are shown in Fig. 6. As discussed in the experimental section, typical experimental scans have been performed for two different incidence angles of 65 and 75°. The experimental data were analyzed by an adjustable parameter model to obtain a viable optical model compromising both microstructural parameters and optical constants of the film. Furthermore, the Tauc-Lorentz oscillator model has been used to describe the optical constants of the material. From the results in Fig. 6, it is clear that the theoretically simulated curves (solid line) agree with the experimental data (depicted using circle) very well and hence the material property can be described accurately. The variations of extinction co-efficient of undoped TiO_2 and 0.5% Ag-TiO_2 are shown in Fig. 7. It is clear the decrease of absorption edge upon increasing Ag doping content is an indication of the decrease of band gap. A similar trend was also observed in our optical absorbance measurements (refer to Fig. 5). The calculated values of band gap are listed in Table 2. In conclusion upon increasing the Ag doping content, it is possible to tune/change/decrease the band gap of TiO_2 which makes this material more attractive

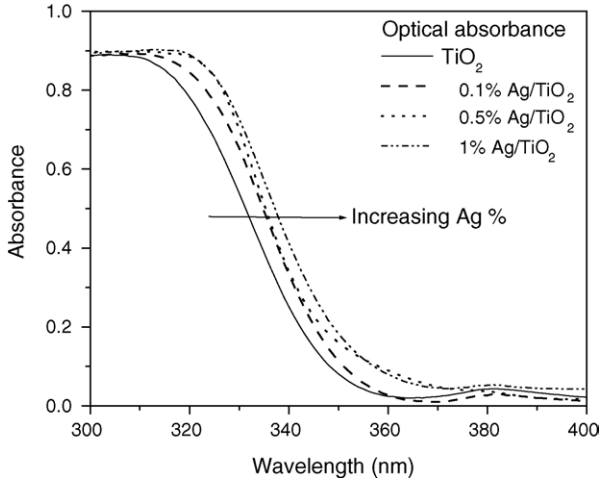

Fig. 5. Optical absorbance spectra of TiO_2 and Ag-TiO_2.

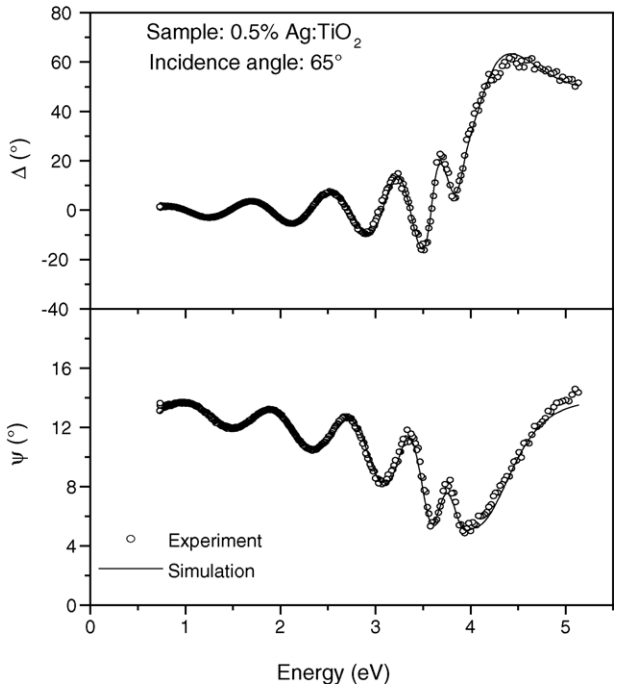

Fig. 6. Typical spectroscopic ellipsometry measurement of 0.5% Ag-TiO_2 together with the theoretical simulations (solid line) as a function of energy. The measurements were carried out for the films coated on microscopic slide. [Ellipsometry parameters del Δ—surface polarized light and psi Ψ—plan polarized light.]

for photocatalytic applications, because the electron–hole pair separation efficiency induced by enhancing the charge pair separation and inhibiting their recombination by the Ag dopant.

It is well known that the photocatalytic activity of TiO_2 depends upon three factors [10]: (i) the electron–hole pair production capacity, (ii) the separation efficiency of the photogenerated charge pair, and (iii) the charge transfer efficiency of the holes and electrons to compounds adsorbed on TiO_2. Chao et al. [10] has reported band gap broadening of the sol–gel prepared TiO_2 films. Upon increasing Ag doping content they observed band gap broadening and it is unfavorable for the photocatalytic activity and they have identified that this is because of anatase grain decrease. But in our Ag-TiO_2 cases the anatase grain increases with increasing Ag dopant and from our optical studies we observed band gap shortening. Because of this band gap shortening, the yield of photogenerated electron–hole pair increases and it is more favorable for photocatalytic activity of TiO_2.

Table 2
Band gap E_g and film thickness value of TiO_2 and Ag-TiO_2 values

Serial number	Percentage of Ag deposited on TiO_2	Film thickness (nm)	Band gap E_g (eV)
1	0	472.65	3.19
2	0.1	358.42	3.21
3	0.5	519.00	3.10
4	1.0	375.75	3.07
5	1.5	464.67	2.96

3.2. Photocatalytic degradation of TCP in aqueous suspension

To evaluate the photocatalytic activity of Ag-TiO_2 and find out the optimum content of Ag impurity, a set of experiments for TCP degradation with an initial concentration of 20 mg L^{-1} under UV-A irradiation was carried out in aqueous suspension using TiO_2 or Ag-TiO_2 catalysts with a Ag content between 0.1 and 2.0 wt%, and the experimental results are shown in Fig. 8. The experimental results demonstrated that after 120 min reaction, TCP in all the suspensions were reduced by more than 95%. Among them, the 0.5% Ag-TiO_2 catalyst achieved the highest efficiency of the TCP degradation. A higher Ag content on TiO_2 seems to be detrimental to the TCP photodegradation efficiency. It was found that the pseudo-first-order kinetics was obeyed for

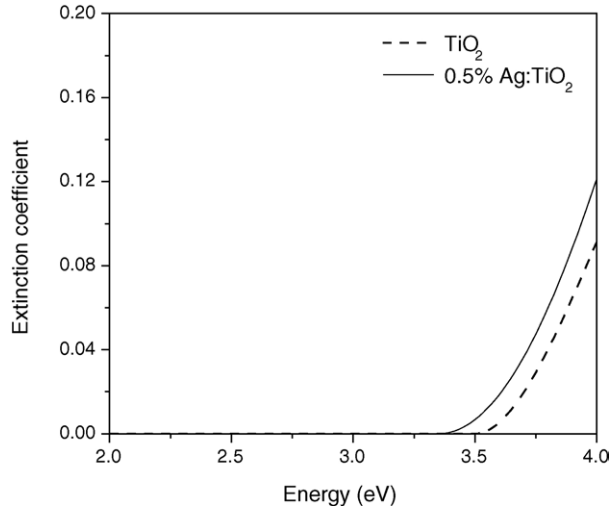

Fig. 7. Variation of extinction coefficient as a function of energy. It is evidenced that upon increasing Ag dopant concentration the absorption edge decreases, band gap decreasing.

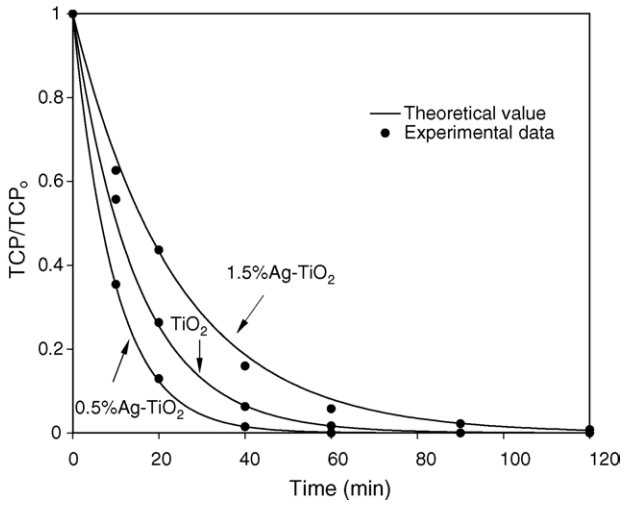

Fig. 8. Kinetics of 2,4,6-trichlorophenol degradation under UV-A irradiation (initial concentration of TCP = 20 mg L^{-1}; pH 5.15; catalyst = 1 g L^{-1}).

Table 3
Apparent kinetic values for the degradation of 2,4,6-trichlorophenol by Ag-TiO_2

Serial number	Name of the catalyst	Kinetic constant (min^{-1})	R^2 value
1	TiO_2	0.0682	0.9990
2	0.1% Ag-TiO_2	0.0931	0.9997
3	0.5% Ag-TiO_2	0.1046	0.9997
4	1% Ag-TiO_2	0.0985	0.9925
5	1.5% Ag-TiO_2	0.0419	0.9892
6	2% Ag-TiO_2	0.0075	0.4778

the photocatalytic degradation of TCP. The calculated kinetic constants are listed in Table 3 and show a maximum value at the Ag content of 0.5 wt%.

From the Fig. 8, the results show that the photocatalytic activity of pure TiO_2 is lower than that of Ag-TiO_2 with Ag content below 1.0 wt%. It implies that the Ag dopant promotes the charge pair separation efficiency for TiO_2 catalysts. It may be explained that at the Ag content below its optimum level, the Ag particles deposited on the TiO_2 surface can act as electron–hole separation centers [17]. The electron transfer from the TiO_2 conduction band to metallic Ag particles at the interface is thermodynamically possible because the Fermi level of TiO_2 is higher than that of Ag metal [24]. This results in the formation of a Schottky barrier at metal–semiconductor contact region and improves the photocatalytic activity of TiO_2. On the contrary, at the Ag content beyond its optimum value, the Ag particles can also act as recombination centers, thereby decreasing the photocatalytic activity of TiO_2. It has been reported that the probability for the hole capture is increased by the large number of negatively charged Ag particles on TiO_2 at high Ag content, which reduces the efficiency of charge separation [25,26]. In this study, the Ag-TiO_2 sample under UV-A irradiation demonstrated a considerable degradation of TCP in aqueous solution.

3.3. Photocatlaytic mineralization of TCP in aqueous suspension

To study the mineralization of TCP in this photocatalytic reaction, the experiment of TCP degradation with initial TOC concentration of around 7 mg L^{-1} was carried out for 120 min and seven samples in each test were collected at the time intervals of 0, 10, 20, 40, 60, 90, and 120 min, respectively and analyzed for TOC concentration. The TOC concentration with an initial value of 7 mg L^{-1} in TCP solution decreased significantly during the photoreaction by using all the prepared photo-catalysts as shown in Fig. 9. It was found that the TOC removals with pure TiO_2, 0.1% Ag-TiO_2, 0.5% Ag-TiO_2, 1% Ag-TiO_2, 1.5% Ag-TiO_2 and 2.0% Ag-TiO_2 were achieved by 66, 78, 79, 75, 53 and 50%, respectively after 120 min reaction. These results indicated that 0.5% Ag-TiO_2 achieved the highest TOC removal, which was also matched with the TCP degradation results.

During the photocatalytic degradation of TCP, dechlorination to convert chlorines into chloride ions is a key step for detoxication. To determine a mass balance for the dechlorination of TCP, chloride ion concentration (Cl^-) was monitored

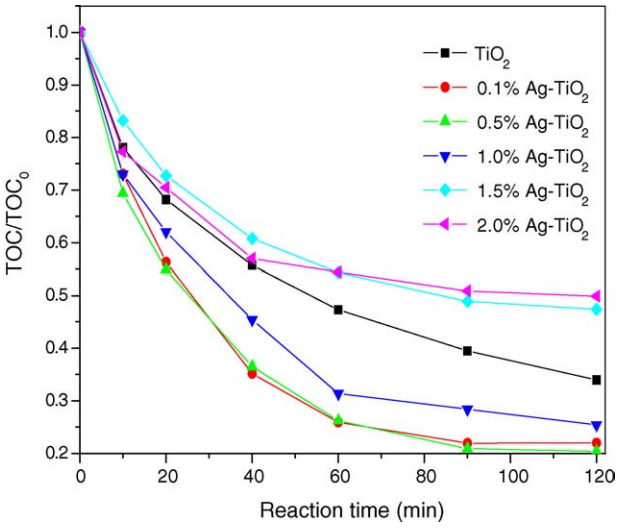

Fig. 9. TOC removal in 2,4,6-trichlorophenol degradation under UV irradiation (initial concentration of TCP = 20 mg L^{-1} and TOC = 7 mg L^{-1}; pH 5.15; catalyst = 1 g L^{-1}).

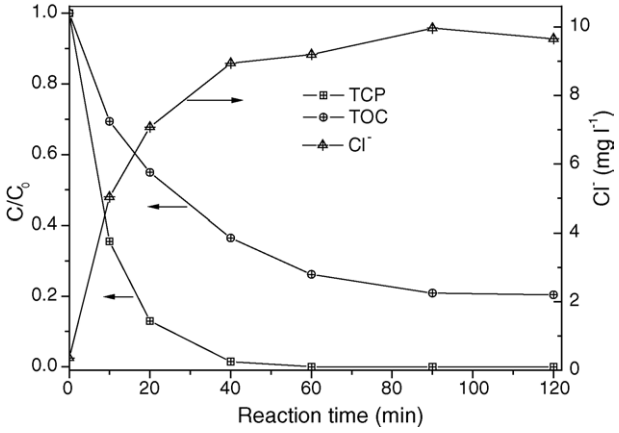

Fig. 10. Variation of of TCP, Cl^-, and TOC concentrations during the mineralisation of 2,4,6-trichlorophenol. (TCP_0 = 20 mg L^{-1}; Cl_0 = 10 mg L^{-1} as Cl_2; TOC_0 = 7 mg L^{-1}).

during TCP degradation. The existent concentration ratios of TCP, TOC and Cl^- versus time are shown in Fig. 10. The results demonstrated that TCP completely disappeared within the 1st h and chloride formation occurred accordingly, but TOC had 20% leftover after 2 h. It is indicated that the TCP degradation and its dechlorination are faster than its mineralization. The decomposition of TCP proceeds a chlorine-released pathway, due to chloride concentration increased when TCP degreased simultaneously. After 1 h, chloride ions were released completely, while TOC still remained, indicating only chlorine-free intermediates and final products in the solution at the end of reaction.

4. Conclusions

In the present work, an enhancement of the photocatalytic activity of TiO_2 catalyst by doping with silver has been confirmed in the degradation of 2,4,6-trichlorphenol as a model pollutant. It was found that with a suitable amount (0.5 wt%),

the Ag dopant effectively increases the photocatalytic activity of the TiO_2. Silver deposits on the TiO_2 surface behave as sites where electrons accumulate. Better separation of electrons and holes on the modified TiO_2 surface, allows more efficient channeling of the charge carriers into useful reduction and oxidation reactions rather than recombination reactions. The experiments demonstrated that TCP was effectively degraded in aqueous Ag-TiO_2 suspension by more than 95% within 120 min, while TOC was also converted into CO_2 by a high portion of up to 80%. The degradation of TCP occurs via chlorine-release pathways. Under UV-A irradiation, however, Ag dopant may exhibit the effect only as electron traps, thus leading to the slight enhancement in the Ag-TiO_2 photocatalytic activity. This study confirms the potential of heterogeneous photocatalysis to purify wastewaters containing aromatic pollutants, particularly chlorinated substances, which are often toxic for microorganism in biological treatments.

Acknowledgement

The authors wish to thank The Hong Kong Polytechnic University for a financial support to carry out this work under a Postdoctoral Fellowship Grant (Project No.: G-YW91/02).

References

[1] F. Serra, M. Trillas, J. Garcia, X. Domenech, J. Environ. Sci. Health. A 29 (7) (1994) 1409.
[2] J. Theurich, M. Lindner, D.W. Bahnemann, Langmuir 12 (1996) 6368.
[3] S. Manahan, Environmental Chemistry, CRC Press, Boca Raton, FL, 1994.
[4] J. Bandara, J.A. Mielczarski, A. Lopez, J. Kiwi, Appl. Catal. B: Environ. 34 (2001) 321.
[5] Ph. Howard, Handbook of Environmental Degradation Rates, Lewis Publishers, MI, 1991.
[6] R. Schwarzenbach, Ph. Gschwend, D. Imboden, Environmental Organic Chemistry, Wiley, New York, 1996.
[7] D.F. Ollis, H. Al-Ekabi, Photocatalytic Purification and Treatment of Water and Air, Elsevier, Amsterdam, 1993.
[8] Y.S. Shen, Y. Ku, Ind. Pollut. Prevent. Control 56 (1995) 278.
[9] A. Mills, R.H. Davies, D. Worsley, Chem. Soc. Rev. 22 (1993) 417.
[10] H. Chao, Y. Yun, H. Xingfang, L. Andre, Appl. Surf. Sci. 200 (2002) 239.
[11] Y. Gao, B. Chen, H. Li, Y. Ma, Mater. Chem. Phys. 80 (2003) 348.
[12] J. Tauc, R. Grigorovic, A. Vancu, Phys. Stat. Solidi 15 (1996) 627.
[13] J. Tauc, in: S. Nudelman, S.S. Mitra (Eds.), Optical Properties of Solids, Plenum, New York, 1969, p. 551.
[14] G.E. Jellison, V.I. Merkulov, A.A. Puretzky, D.B. Geohegan, G. Eres, D.H. Lowndes, J.B. Caughman, Thin Solid Films 68 (2000) 377.
[15] J.A. Woolam Co. Inc., Guide to Using WASE32™ (WexTech, New York, 1995), p. 269.
[16] S. Venkataraj, O. Kappertz, R. Drese, Ch. Leisch, R. Jayavel, M. Wuttig, Phys. Stat. Solidi (a) 194 (2002) 192.
[17] J.M. Hermann, H. Tahiri, Y. Ait-Ichou, G. Lassaletta, A.R. Gonzalez-Elipe, A. Fernandez, Appl. Catal. B: Environ. 13 (1997) 219.
[18] I.R. Bellobono, A. Carrara, B. Barni, A. Gazzotti, J. Photochem. Photobiol. A 84 (1994) 83.
[19] D. Mardare, M. Tasca, M. Delibas, G.I. Rusu, Appl. Surf. Sci. 156 (2000) 200.
[20] J. Liu, J.C. Yu, D. Lo, S.K. Lam, J. Catal. 183 (1999) 368.
[21] F. Liang-rong, L. Chao-jie, Q. Fa-li, Acta Chim. Sin. 60 (3) (2000) 463.
[22] D. Briggs, M.P. Seah, Practical Surface Analysis, Wiley, New York, 1983.
[23] T. Sano, N. Negishi, K. Uchino, J. Tanaka, S. Matsuzawa, K. Takeuchi, J. Photochem. Photobiol. A 160 (2003) 93.
[24] A. Scalfani, J.M. Hermann, J. Photochem. Photobiol. A 113 (1998) 181.
[25] V. Vamathevan, R. Amal, D. Beydoun, G. Low, S. McEvoy, J. Photochem. Photobiol. A 148 (2002) 233.
[26] X.Z. Li, F.B. Li, Environ. Sci. Technol. 35 (2001) 2381.